

Adsorption of Weak Polyelectrolytes on Metal Oxide Surfaces: A Hybrid SC/SF Approach

KWOK-KEUNG AU, SHUOLIN YANG, AND CHARLES R. O'MELIA*

Department of Geography and Environmental Engineering,
The Johns Hopkins University, Baltimore, Maryland 21218

A hybrid SC/SF model to describe the adsorption of weak polyelectrolytes on metal oxide surfaces is presented. This model couples the surface complexation (SC) model for the effects of surface and solute speciation on the adsorption of monomers on oxides with the Scheutjens–Fleur (SF) model for the effects of macromolecular properties on the adsorption of polymers and polyelectrolytes on surfaces. The average magnitude of the specific interactions between polyelectrolyte functional groups and surface sites, expressed by the parameter $\chi_s(\text{hyb})$, varies systematically with surface and polyelectrolyte speciation and hence with solution chemistry. Measurements of the adsorption of polygalacturonic acid (PGUA) on hematite over wide ranges of pH and ionic strength are used to test the hybrid model. Good agreement of model simulations and adsorption measurements is achieved. A reaction represented by $\text{>MeOH} + \text{L}^- = \text{>MeOHL}^-$ provides the best representation of the experimental data.

Introduction

The objectives of this research are three in number: (a) to extend present theoretical frameworks for the adsorption of weak polyelectrolytes on metal oxide surfaces, (b) to test this new approach experimentally, and (c) based on these theoretical and experimental results, to provide a better understanding of the adsorption process.

Due to its scientific interest and technological importance, the adsorption of weak polyelectrolytes on metal oxide surfaces in aquatic environments has received increasing attention (1–6). An important application arises from the macromolecular character of natural organic matter (NOM) (7). The adsorption of weak polyelectrolytes provides a useful framework for describing the adsorption behavior of NOM (4, 8).

The adsorption of polymers and polyelectrolytes is influenced to a great extent by their size. Macromolecules lose conformational entropy when they adsorb to any surface. An enthalpic compensation must exist for adsorption to occur (9). In many cases, anionic polyelectrolytes and NOM can adsorb on surfaces with negative charge (2, 6, 10). This suggests that driving forces other than electrostatic interactions between polyelectrolytes and surfaces are important. Specific (nonCoulombic) interactions between polyelectrolyte functional groups and surface sites are often proposed (1, 3, 10). Other mechanisms are possible, such as specific electrolyte effects. These effects originate from specific

adsorption of salt ions on the surfaces and/or nonCoulombic interactions of these ions with the polyelectrolytes. Such specific interactions can reduce the negative charges of the surfaces and/or the polyelectrolytes and thus enhance adsorption (11). To model the adsorption of weak polyelectrolytes on oxide surfaces, a theory with emphasis on the specific interactions between polyelectrolyte functional groups and oxide surface sites and on the macromolecular nature of polyelectrolytes is developed and tested herein. Specific electrolyte effects are not addressed.

Experimental Methods

Hematite ($\alpha\text{-Fe}_2\text{O}_3$) particles, a representative of iron oxides in natural aquatic systems, were used as the adsorbent. The hematite particles were synthesized according to the procedure of Penners (12). The resulting particles were approximately spherical and nearly monodisperse with a diameter of $96 (\pm 8.9)$ nm as determined by transmission electron microscopy (TEM). Acid–base titrations were performed to determine the surface charge density (σ_0 , coul/m²) of the hematite particles at different pHs and NaNO₃ concentrations. The point of zero charge (pH_{pzc}) of the hematite was observed to be 8.1.

Polygalacturonic acid (PGUA) was used as the adsorbate. PGUA is a chemically well defined, linear anionic polysaccharide. It was obtained from Fluka CHEMIE AG. PGUA contains carboxyl groups and may be considered as a surrogate for NOM. The PGUA used in this research is monodisperse and has a weight average molecular weight of $54\,700 (\pm 4700)$ g/mol as determined by static light scattering. Acid–base titrations were performed to determine the charge density (σ_p , coul/mg C) of PGUA at different pHs and NaNO₃ concentrations. The intrinsic acidity constant (pK_a(int)) for PGUA was 3.92 as determined from a Henderson–Hasselbalch plot (13) using the acid–base titration data.

All other chemicals were analytical grade. Stock solutions were prepared with distilled, deionized, filtered water and then passed through 0.22 μm Millipore filters to remove particles.

Adsorption densities (Γ , mg/m²) were determined at different pHs and NaNO₃ concentrations (14). High concentrations of hematite (750 mg/L) and PGUA (250 mg/L) were used to ensure that Γ could be measured accurately and the adsorption plateau levels were reached. Samples with the desired concentrations of PGUA and NaNO₃ were prepared, and the pH was adjusted to the desired value. Hematite particles were then added to the samples and pH was readjusted. An individual sample was prepared for each solution condition to minimize hysteresis upon cycling pH or salt concentration. Γ was obtained by taking the difference between the PGUA concentration remaining in solution in blanks containing no hematite and samples containing hematite after 24 h of equilibration time followed by centrifugation. PGUA concentrations were measured using a total organic carbon (TOC) analyzer. A more detailed description of the experimental methods is given by Yang (14).

SF Theory

Theoretical Basis. SF theory and its extensions by Scheutjens, Fleur, and co-workers (15–18) are a milestone in modeling the adsorption of polymers and polyelectrolytes on solid surfaces. A detailed discussion of SF theory is given by Fleur et al. (19). SF theory has been used to evaluate and predict the equilibrium behavior of polymers and polyelec-

* Corresponding author phone: (410)516-7102; fax: (410)516-8996; e-mail: omelia@jhuvms.hcf.jhu.edu.

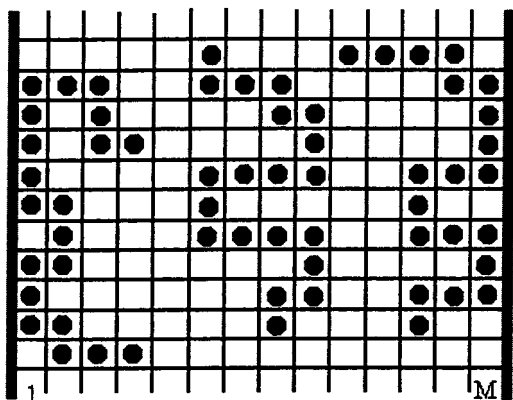


FIGURE 1. Lattice representation of polyelectrolytes adsorbed and in solution between two surfaces.

trolytes on uncharged and oppositely charged surfaces (15–21). The Böhmer version of SF theory (17) for the adsorption of weak polyelectrolytes on charged surfaces is used in this research.

SF theory is a statistical thermodynamic lattice model. The solid/liquid interface is described by a lattice having M layers. A schematic picture of this system containing two adsorbent surfaces, two adsorbed polyelectrolyte molecules (one adsorbed to each surface), and one polyelectrolyte molecule in bulk solution is shown in Figure 1. The adsorbent surfaces are the infinite flat plate boundaries of the lattice and are characterized by either a surface charge (σ_0) or a surface potential (ψ_0 , mV). σ_0 and ψ_0 are placed at a plane separated from the closest polyelectrolyte adsorption plane by a short distance. It is assumed that either σ_0 or ψ_0 remains constant during adsorption. This assumption has been removed in a new version of SF theory (18) but is retained in this research. A multicomponent system containing polyelectrolytes, water, H^+ , OH^- , and monovalent ions is considered. Each polyelectrolyte molecule is treated as an assembly containing r segments or statistical units, while each molecule or ion of all other species is considered to consist of one segment.

Two types of parameters are used to describe the nonelectrostatic (specific) interactions among all species including the surfaces. Nonelectrostatic interactions between any two segment types x and y are characterized by a Flory–Huggins parameter, $\chi_{y,x}$ (units of kT) (22). Nonelectrostatic interactions between a segment x and a surface site s are characterized by a parameter $\chi_{s,x}$ after Silberberg (23). $\chi_{s,x}$ is defined as the nonelectrostatic part of the energy change (units of kT) of an exchange process in which a segment x adsorbed to the surface is exchanged for a solvent (water) molecule in the solution. $\chi_{s,x}$ is positive if segment x adsorbs preferentially from the solvent. It is assumed in the Böhmer version of SF theory that all surface sites have the same $\chi_{s,x}$.

For specific interactions between polyelectrolyte functional groups and surface sites, this parameter is abbreviated as χ_s in the remainder of this paper. In existing studies, χ_s is often used as a fitting parameter, and a single constant value of χ_s has been used in modeling adsorption at different pHs and ionic strengths (17–21).

At equilibrium, the distributions of adsorbed polyelectrolytes and all other species are determined by conformational entropy effects, enthalpic effects, and excluded volume effects. These distributions are subjected to a self-consistent mean potential field. The resulting potential energy field for segment x in layer i , $u_x(i)$ (units of kT), is given in

$$u_x(i) = u_x^{\text{nel}}(i) + u_x^{\text{el}}(i) + u'(i) \quad (1)$$

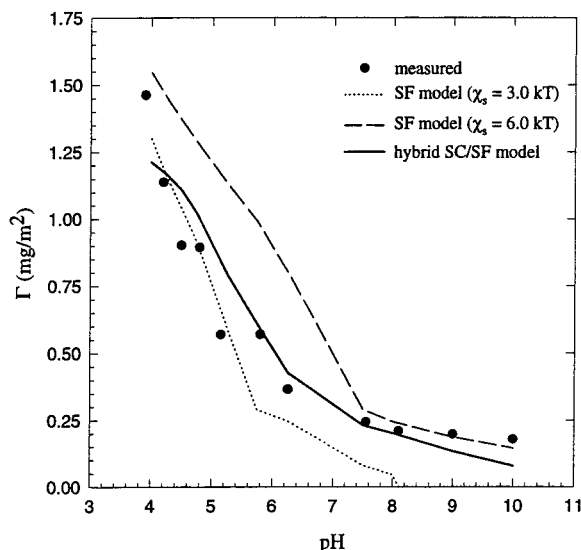


FIGURE 2. Experimental and simulated values of Γ for PGUA (250 mg/L) adsorbed on hematite (750 mg/L) as a function of pH at an I of 0.01 (background electrolyte $NaNO_3$). Experimental results are from Yang (14). In the SF modeling results, two different values of χ_s are used. In the hybrid SC/SF modeling results, the values of χ_s (hyb) are based on reaction 6. A value of 5.6 kT is used as a baseline to fit Γ at pH 8.0. All other simulation parameters are shown in Tables 1 and 2. Modeling results are converted from equivalent monolayers to mg/m^2 based on the molecular weight and size of a PGUA segment ($1 \text{ mg/m}^2 = 0.88$ monolayers).

Here $u_x^{\text{nel}}(i)$ is the contribution of nonelectrostatic interactions and expressed by

$$u_x^{\text{nel}}(i) = -\chi_{s,x} + \sum_y \chi_{y,x} (\langle \phi_y(i) \rangle - \phi_y^b) \quad (2)$$

The first term on the right side of eq 2 is the contribution from the nonelectrostatic interactions between segment x and the surface. This term is only used in the layers immediately adjacent to the surfaces (the first and the M th lattice layers). It is affected by the modification to the model addressed later in this paper. The second term arises from the nonelectrostatic interactions between segment x and all other segments. $\phi_y(i)$ and ϕ_y^b are the volume fractions of segment y in layer i and in bulk solution, respectively. $\langle \rangle$ is the notation representing the weighted average of the volume fraction over three adjacent lattice layers.

$u_x^{\text{el}}(i)$ is the electrostatic contribution for charged segments and is treated coulombically. Coulombic interactions and the charge/electric potential relationships at the interfaces are handled by a multilayer model with the Poisson–Boltzmann equation describing variation of electric potential between layers. Finally, $u'(i)$ represents the excluded volume effects.

For species having only one segment (e.g. Na^+), the local volume fraction is related to $u_x(i)$ by a Boltzmann factor. For polyelectrolytes, a random walk Markov process in the lattice is used to account for the interconnection between segments within a chain. Results from SF theory include a detailed description of the conformations of adsorbed polyelectrolytes and the electrostatic structure at the interfaces.

Experimental and Modeling Results. Experimental and SF modeling results of Γ for PGUA adsorbed on hematite using two different values of χ_s (3.0 and 6.0 kT) at an ionic strength (I) of 0.01 are shown in Figure 2. All other simulation parameters are given in Tables 1 and 2. Simulation results using the hybrid model developed later in this paper are included in this figure and discussed in the last section.

TABLE 1. Input Parameters Used in Adsorption Modeling

surface charge ^b	varies						
lattice ^c	type	hexagonal					
	size (nm)	0.5					
	no. of layers	80					
species		PGUA	H ⁺	OH ⁻	Na ⁺	NO ₃ ⁻	H ₂ O
	r_x^d	310	1	1	1	1	1
	v_x^e	-1	+1	-1	+1	-1	0
	ϵ_x^e	20	80	80	80	80	80
PGUA	$pK_a(\text{int})^f$	3.92					
	bulk concn ^g (vol fraction)	2.5×10^{-4}					
pH	varies						
salt concn (M)	varies						

^a $\chi_{s,x}$ and $\chi_{y,x}$ are listed in Table 2. All simulations were performed on a 3-node Vaxcluster computer using a computer program written in FORTRAN. ^b Surface charge is input from measured data of hematite in the absence of PGUA by Yang (14) (shown in Figure 3a). ^c Lattice size is taken from Yang (14) which is based on measurement of crystal dimension of galacturonic acid using X-ray diffraction by Hjortas et al. (24). ^d r_x is the number of segments that each molecule or ion has. r for PGUA is based on the molecular weight of PGUA molecules and the molecular weight of a PGUA segment. ^e v_x is valence and ϵ_x is relative dielectric permittivity of segment x . ^f $pK_a(\text{int})$ is estimated with a Henderson-Hasselbalch plot based on acid-base titration of PGUA (14). ^g Bulk concentrations of H⁺ and OH⁻ are determined by pH; bulk concentration of Na⁺ and Cl⁻ are determined by salt concentration; bulk concentration of H₂O is calculated such that the sum of the volume fractions of all species equals 1.

TABLE 2. Nonelectrostatic Interaction Parameters ($\chi_{s,x}$ and $\chi_{y,x}$) Used in Adsorption Modeling (Units of kT)

species ^a	$\chi_{s,x}$	$\chi_{y,x}$					
		PGUA	H ⁺	OH ⁻	Na ⁺	NO ₃ ⁻	H ₂ O
PGUA	varies	0	0	0	0	0	0.5
H ⁺	0	0	0	0	0	0	0
OH ⁻	0	0	0	0	0	0	0
Na ⁺	0	0	0	0	0	0	0
NO ₃ ⁻	0	0	0	0	0	0	0
H ₂ O	0	0.5	0	0	0	0	0

^a All species except PGUA are considered indifferent to the surface and thus their $\chi_{s,x}$ is assumed to be 0. Surface hydroxyl groups are formed by specific adsorption of H⁺/OH⁻ on hematite surfaces; these effects are accounted for by a measured surface charge (σ_0) of hematite at a given pH and I . ^b $\chi_{y,x}$ between PGUA segments and water molecules is taken to be 0.5. The net $\chi_{y,x}$, after accounting for the electrostatic repulsion between charged PGUA segments, is thus less than 0.5. This reflects the fact that water is a good solvent for PGUA. All other $\chi_{y,x}$ are taken to be 0, equivalent to assuming that there are no net specific interactions among these species. Although H⁺ reacts with PGUA, this is handled by an acidity constant (K_a).

Measurements of Γ decrease with increasing pH. Over the broad range of pH, there is mutual electrostatic repulsion between charged PGUA segments. The negative charge density of PGUA increases with increasing pH and so do these repulsions. This partly accounts for the observed trend in Γ . An electrostatic interaction between charged PGUA segments and hematite also exists. This interaction is attractive at pH < 8.1 where the hematite is positively charged and is repulsive at pH > 8.1 where the hematite is negatively charged. This electrostatic interaction between charged PGUA segments and hematite contributes to the high Γ at low pH and also to the low Γ at high pH. However, electrostatic effects alone cannot explain the adsorption at pH > 8.1. As it is unlikely that the background electrolyte, NaNO₃, reacts with hematite and/or PGUA specifically, specific electrolyte effects are probably negligible. Furthermore, hydrophobic interactions are expected to be small or absent for PGUA. NonCoulombic interactions between PGUA and surface sites are probably involved in the adsorption. These interactions are also termed specific or chemical interactions in this paper.

Specific interactions between hematite and PGUA are included in the simulations by the fitting parameter χ_s . With a χ_s of 3.0 kT, the model describes Γ at low pH but underestimates it at high pH. More significantly, this χ_s leads to the prediction that there is essentially no adsorption at pH > pH_{pzc}. This could be a major problem in application

because most particles in natural aquatic systems have a negative charge. Use of a χ_s of 6.0 kT predicts significant adsorption at pH from 7.5 to 10.0. However, its use also results in significant overestimation of Γ at pH less than 7.0.

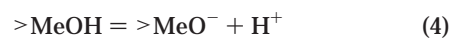
These comparisons between measured and simulated results indicate that a single constant value of χ_s does not describe Γ accurately over a broad range of pH. It is hypothesized in this paper that the specific chemistry of the interactions between the polyelectrolytes and surfaces is not addressed adequately in the SF model. Operationally, the SF model can be used to fit Γ by using values of χ_s that vary with pH. The basis of this variation, including a theoretical framework, is the focus of this paper.

Hybrid SC/SF Model

Surface Complexation Model and Speciation. A seminal contribution in describing surface speciation and adsorption properties of metal oxides in aquatic environments is the surface complexation (SC) model by Schindler, Stumm, and co-workers (25–30). When applied directly to the adsorption of polyelectrolytes on oxide surfaces, the SC model does not account for the macromolecular nature of the polyelectrolytes. In contrast, the SF model for polyelectrolyte adsorption does not address specific ligand and surface site interactions. A hybrid model is developed herein to combine the SC and SF models to include the strengths of both approaches.

In the SC model, adsorption on oxide surfaces is treated as chemical reactions between surface sites and sorbing substances. Site binding models are used to describe the reaction stoichiometries. Electrostatic models are used to specify the structure of the resulting electric double layer and its electrostatic effects on these reactions.

Different approaches can be used to characterize the oxide surface groups. Two common approaches are the single site model (29) and the multisite model (31). The single site model is used in this research. This is because it is simpler and can account qualitatively and quantitatively for many experimental data in the literature. In the absence of other specifically adsorbing substances, the reaction of protons with neutral surface hydroxyl groups (>MeOH) induces surface charge according to the following reactions:



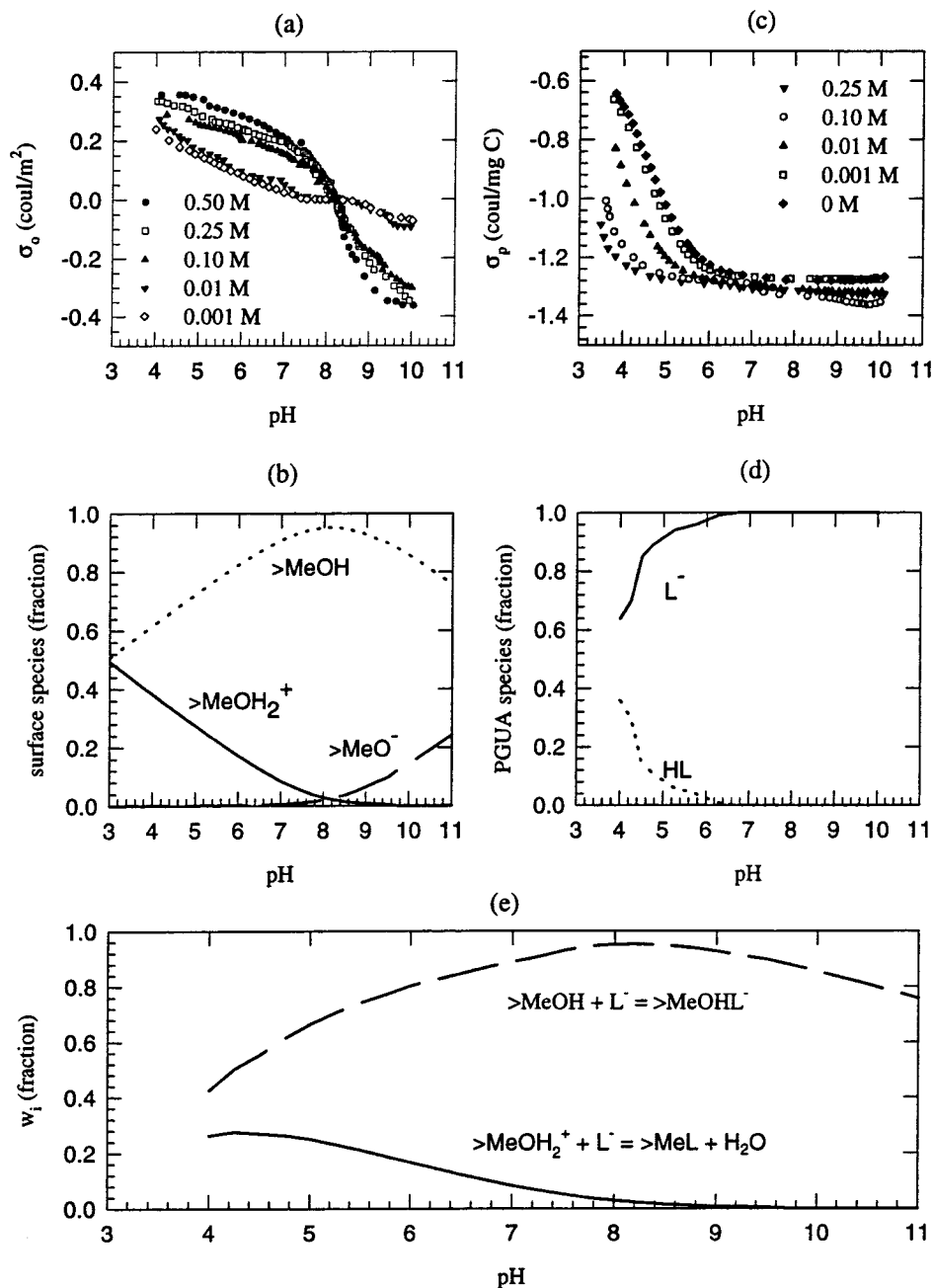


FIGURE 3. (a) Measured σ_o of hematite as a function of pH at different NaNO₃ concentrations from Yang (14). (b) Simulated surface speciation of hematite as a function of pH at an I of 0.01. Constant capacitance model (site density 4 site/nm², capacitance 1.5 F/m², $\text{p}K_{a1}^s(\text{int})$ 6.5, $\text{p}K_{a2}^s(\text{int})$ 9.7). (c) Measured σ_p of PGUA as a function of pH at different NaNO₃ concentrations from Yang (14). (d) Calculated speciation of PGUA as a function of pH at an I of 0.01. (e) Calculated w_i for reactions 6 and 7 as a function of pH at an I of 0.01 ($w_6 = f_6f_L$, $w_7 = f_1f_L$).

Measurements of σ_o of hematite in the absence of PGUA are presented in Figure 3a (14). Simulated surface speciation of hematite at an I of 0.01 using a SC model is presented in Figure 3b. A constant capacitance model (27) is used to describe the electrostatic interaction. Simulation parameters are chosen to fit the measured σ_o over the broad range of pH at this I . The computer program HYDRAQL (32) was used to perform the calculations. The fraction of $>\text{MeOH}$ surface groups (f_6) increases with increasing pH at pH < 8.1 and decreases with increasing pH at pH > 8.1. The fraction of $>\text{MeOH}_2^+$ surface groups (f_1) decreases with increasing pH, and the fraction of $>\text{MeO}^-$ surface groups (f_{-1}) increases with increasing pH.

The constant capacitance model can be applied at other ionic strengths, although the parameters used to fit mea-

surements of σ_o at other ionic strengths may be different. The result (not shown) is that, at a given pH, the dominant charged species ($>\text{MeOH}_2^+$ at pH < 8.1, $>\text{MeO}^-$ at pH > 8.1) increase with increasing I , while the neutral species ($>\text{MeOH}$) decreases with increasing I .

The dissociation of weak polyacids in solution is illustrated by the following reaction:



Here HL and L^- represent undissociated and dissociated species of the weak polyacid. The measured values of σ_p of PGUA are shown in Figure 3c (14). PGUA speciation in solution is calculated based on these data. The results at an I of 0.01 are shown in Figure 3d. In these calculations, the

fraction of PGUA segments that is dissociated (f_i) is the ratio of σ_p at a particular pH to the maximum measured σ_p . The latter is -1.36 coul/mg C, in agreement with the maximum σ_p calculated from the chemical structure and molecular weight of the PGUA. f_i increases with increasing pH until $f_i = 1.0$. A similar procedure can be applied at other ionic strengths. The result (not shown) is that, at a given pH, f_i increases with increasing I and can reach a maximum value of 1.0 at neutral pH or higher.

These results indicate that solution chemistry affects both surface and polyelectrolyte speciation significantly; pH shifts the acid–base equilibria and ionic strength changes the electrostatic interactions involved in these reactions.

Adsorption of weak polyelectrolytes on metal oxide surfaces is considered to involve a chemical reaction between one type of polyelectrolyte species and one type of proton-reactive surface species. Different adsorption reactions are possible representations of this process. The following reactions with 1:1 stoichiometry are considered:



It is assumed in SF theory that each surface site has the same χ_s regardless of the different surface groups and segment types that may exist. This is equivalent to assuming an average interaction parameter taken over all surface and polyelectrolyte species. The variations in surface and polyelectrolyte speciation by solution chemistry can have effects on χ_s and thus on simulations of polyelectrolyte adsorption. An analysis to address the effects of speciation on χ_s follows.

Coupling the SC and SF Models. For each reaction i as illustrated by eqs 6 and 7, let us assume that there is a corresponding segment/surface nonelectrostatic interaction parameter termed χ_{si} . We consider first a simple case in which reaction 6 is the only adsorption reaction with a nonzero χ_{si} . Let us also assume that all polyelectrolyte segments in solution are dissociated ($f_i = 1.0$). f_o can be considered as the probability that a surface site is $>\text{MeOH}$. If $f_i = 1.0$, f_o is also the probability that a surface site can follow reaction 6 and has a nonzero χ_{si} . If an average χ_s is assigned to all surface sites, this average χ_s would be

$$\chi_s = f_o \chi_{si} \quad \text{for } f_i = 1.0 \quad (8)$$

Next let us consider a more general situation in which not all polyelectrolyte segments in solution are dissociated. The probability that a surface site can follow reaction 6 is then a joint probability that a surface site is $>\text{MeOH}$ and a polyelectrolyte segment is L^- , that is the product $f_o f_i$. This product is termed w_i in general and w_6 for reaction 6. Consequently, the average χ_s becomes

$$\chi_s = f_o f_i \chi_{si} = w_i \chi_{si} \quad (9)$$

Similarly, the joint probability that a surface site can follow reaction 7 is the product $f_i f_i$ and termed w_7 .

χ_{si} is a constant regardless of the changes in pH and ionic strength. However, f_o , f_i , and f_i depend on solution conditions. w_6 and w_7 at an ionic strength of 0.01 are shown in Figure 3e. w_6 increases with increasing pH at pH < 8.1 and then decreases with increasing pH at pH > 8.1. Except from pH 4.0 to 4.25, w_7 decreases with increasing pH. These changes in speciation affect the average interaction parameter χ_s .

The following relationship between χ_s at any two different solution conditions A and B (e.g., two different pHs or two different ionic strengths) can be obtained:

$$\left[\frac{\chi_s}{f_o f_i} \right]_A = \left[\frac{\chi_s}{f_o f_i} \right]_B \quad \text{for reaction 6} \quad (10)$$

Similarly, the following equation is obtained for reaction 7:

$$\left[\frac{\chi_s}{f_i f_i} \right]_A = \left[\frac{\chi_s}{f_i f_i} \right]_B \quad \text{for reaction 7} \quad (11)$$

If χ_s at one solution condition is known (as a fitting parameter, for instance), then χ_s at all other different solution conditions can be estimated based on the species distributions of the reactants at these different solution conditions. χ_s obtained with this approach is termed $\chi_s(\text{hyb})$.

In using $\chi_s(\text{hyb})$ to calculate polyelectrolyte adsorption with the hybrid SC/SF model, a few limitations should be realized. First, only one reaction is assumed to represent the adsorption. Second, surface and solute speciation before adsorption proceeds are used to estimate $\chi_s(\text{hyb})$. Third, besides the adsorbed species and water, there are no other products (such as H^+ , OH^-).

Results and Discussion

Useful improvements have been attempted in the hybrid model. These improvements include the following (a) the specific chemistry of polyelectrolyte/surface interactions is considered, (b) important effects of surface and solution chemistry on χ_s can be estimated, and (c) information related to the adsorption reaction is obtained.

Γ for PGUA adsorbed on hematite was simulated with the hybrid SC/SF model. The simulation procedure includes (a) determination of speciation of hematite and PGUA before adsorption proceeds (e.g., Figure 3a–d), (b) calculation of w_i for two reactions (e.g., Figure 3e), (c) estimation of $\chi_s(\text{hyb})$ at different solution conditions using a baseline χ_s (defined subsequently) and eq 10 or 11, and (d) simulation of Γ using $\chi_s(\text{hyb})$.

Effects of pH. Values of $\chi_s(\text{hyb})$ for reactions 6 and 7 at an I of 0.01 are shown in Figure 4a. Also shown are $\chi_s(\text{exp})$, the values of χ_s that fit the experimental Γ shown in Figure 2. In the calculation of $\chi_s(\text{hyb})$, a value of 5.6 kT was used as a baseline χ_s to fit Γ at pH 8.0. This pH was chosen to minimize electrostatic interactions between PGUA and hematite surface.

$\chi_s(\text{exp})$ increases with increasing pH, indicating that the average magnitude of chemical interactions between PGUA functional groups and hematite surface sites increases with increasing pH. This can be due to increases in the number of reactive surface sites and/or reactive PGUA species as pH increases. These effects of pH on χ_s are not considered by SF model but are incorporated into the hybrid SC/SF model as illustrated later in this paper.

Comparison of $\chi_s(\text{exp})$ and $\chi_s(\text{hyb})$ indicates that reaction 6 provides good agreement with $\chi_s(\text{exp})$. At pH < 8.1, $\chi_s(\text{hyb})$ increases with pH. This is due to the increases in both $>\text{MeOH}$ surface groups (Figure 3b) and L^- species (Figure 3d) as pH increases. At pH > 8.1, $\chi_s(\text{hyb})$ decreases slightly with increasing pH. This arises from the reduction in $>\text{MeOH}$ surface groups as $>\text{MeO}^-$ surface groups are formed (Figure 3b). In contrast, the values of $\chi_s(\text{hyb})$ based on reactions 7 show poor agreement with $\chi_s(\text{exp})$; $\chi_s(\text{hyb})$ and $\chi_s(\text{exp})$ show opposite trends with pH. $\chi_s(\text{hyb})$ decreases with increasing pH, due to the reduction in $>\text{MeOH}_2^+$ surface groups as pH increases.

Simulations of the adsorption of PGUA on hematite using $\chi_s(\text{hyb})$ based on reaction 6 are shown in Figure 2. At pH < 8.1, fairly good agreement between experimental results and the hybrid model predictions is observed. At pH > 8.1, PGUA adsorption is predicted by the model but to a lesser extent than observed. The discrepancy between predicted and

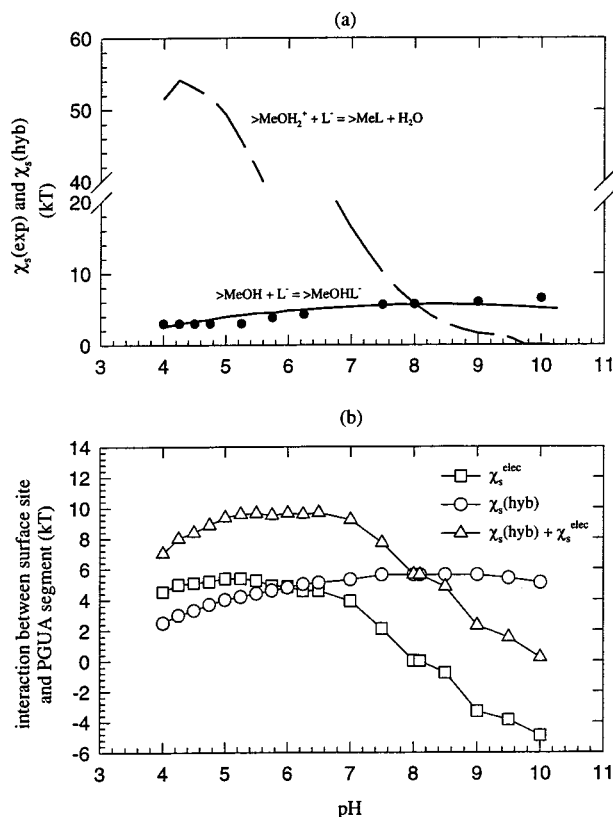


FIGURE 4. (a) $\chi_s(\text{hyb})$ using reactions 6 and 7, and $\chi_s(\text{exp})$ (●) as a function of pH at an I of 0.01. A value of 5.6 kT is used as a baseline to fit Γ at pH 8.0. (b) Interactions between hematite surface sites and PGUA segments as a function of pH at an I of 0.01. χ_s^{elec} is calculated using eq 12 with $\psi(1)$ obtained from σ_0 for hematite. f_L is based on measurements of σ_p for PGUA and equals the fraction of dissociated species as shown in Figure 3d. The values of $\chi_s(\text{hyb})$ are the same as shown in (a) for reaction 6.

measured adsorption densities can be due to assumptions made in the hybrid model or experimental error. However, the hybrid SC/SF model provides better agreement with observations of Γ than an approach that uses any single constant value of χ_s . This is a significant improvement since a broad range of pHs including both similarly and oppositely charged cases are covered in this test.

Adsorption of PGUA on hematite is affected by both electrostatic and specific interactions between PGUA functional groups and surface sites. A term called χ_s^{elec} is defined here to represent the electrostatic interaction between PGUA charged segments and hematite surfaces:

$$\chi_s^{\text{elec}} = -\frac{vef_L\psi(1)}{kT} \quad (12)$$

Here χ_s^{elec} is the negative of the electrical work to transport a segment with a degree of dissociation f_L from the bulk solution to the closest adsorption plane (the first lattice layer) at which an electric potential $\psi(1)$ exists. e is the elementary charge. $\psi(1)$ is chosen because χ_s is also defined based at the first layer. A positive value of χ_s^{elec} represents an attraction between the surface and polyelectrolyte segments.

Results for χ_s^{elec} at an I of 0.01 are shown in Figure 4b. In the calculation of χ_s^{elec} , f_L equals the fraction of dissociated species shown in Figure 3d. $\psi(1)$ refers to the electric potential at the first lattice layer for the hematite and is calculated using the SF model with the assumption that there is no polyelectrolyte in the system. Adsorption of polyelec-

trolytes would change $\psi(1)$. As adsorption of anionic polyelectrolytes proceeds, $\psi(1)$ becomes less positive, making χ_s^{elec} less positive (less favorable). In this and subsequent calculations, χ_s^{elec} thus refers to the initial electrostatic interactions between charged PGUA segments and surfaces. Also shown is $\chi_s(\text{hyb})$ used to simulate Γ as shown in Figure 2. The sum of χ_s^{elec} and $\chi_s(\text{hyb})$, which may be considered as a combined (including Coulombic effects) adsorption energy between a PGUA segment and a surface site, is also shown in this figure. It should be realized, however, that adsorption is determined not only by this combined adsorption energy but also by other factors such as conformational entropy and excluded volume effects.

As expected, χ_s^{elec} is attractive at pH < 8.1 and is repulsive at pH > 8.1. χ_s^{elec} increases with increasing pH from 4.0 to 5.3, due to the rapid increase of σ_p in this pH region even though σ_0 and $\psi(1)$ decrease. At pH > 5.3, χ_s^{elec} decreases with increasing pH. This is mainly due to the deprotonation of surface groups, making σ_0 less positive as pH increases.

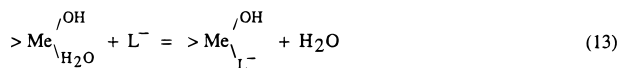
$\chi_s(\text{hyb})$ can vary with solution pH and has been presented in Figure 4a. The sum of $\chi_s(\text{hyb})$ and χ_s^{elec} increases with increasing pH up to a maximum of 9.7 kT at pH 6.5, mainly as a result of increasing $\chi_s(\text{hyb})$ with increasing pH. Since Γ decreases with increasing pH, adsorption under these conditions is probably limited by the lateral electrostatic repulsion among adsorbed polyelectrolyte charged segments.

At pH > 6.5, the sum of $\chi_s(\text{hyb})$ and χ_s^{elec} decreases with increasing pH, mainly due to the decrease in χ_s^{elec} as pH increases. At pH > 8.1, only a small combined adsorption energy between polyelectrolyte segments and surface sites exist. In this pH range, Γ decreases with increasing pH because of the lateral repulsion among charged polyelectrolyte segments and also the decrease in the combined adsorption energy between the surface and polyelectrolyte segments.

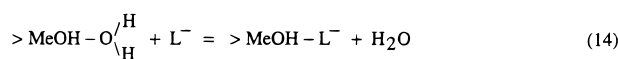
Both electrostatic and specific attractions between PGUA segments and hematite surfaces sites are driving forces for adsorption at pH < 8.1. Their contributions vary with pH. The contribution by specific interaction becomes more important as pH increases. At pH > 8.1, specific interaction is the main mechanism for PGUA adsorption on hematite.

Implications for Adsorption Mechanisms. Results with the hybrid model indicate that eq 6 can describe the adsorption reaction. The actual adsorbed species can only be obtained from molecular level measurements. Several molecular studies of the adsorption of ligands with carboxyl groups on metal and mineral oxides suggest specific interactions between ligands and surface sites as the adsorption mechanism (33–35).

At least two possibilities may be speculated for reaction 6. First, it may be considered as a ligand exchange process, in which L^- replaces a water molecule adsorbed chemically to a surface metal that is also bound to a hydroxyl group, coordinating with the surface metal. This is represented by the following equation



Alternatively, reaction 6 may be viewed as a process in which L^- replaces a water molecule adsorbed physically/chemically to a surface hydroxyl group and is then linked to the $>\text{MeOH}$. Hydrogen bonding may be involved in this linkage. This reaction is represented by the following equation:



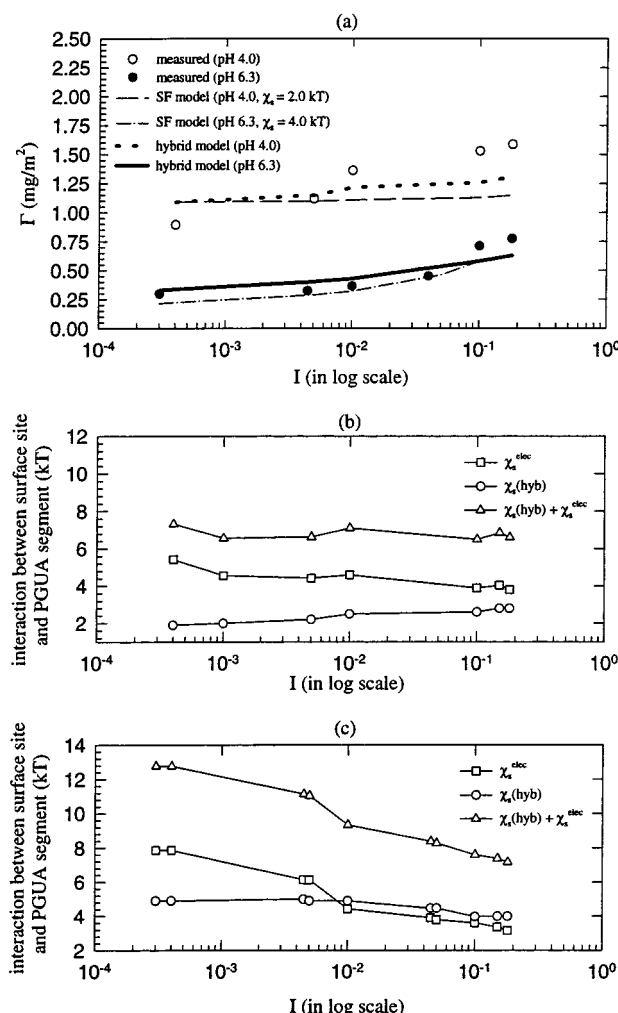


FIGURE 5. (a) Simulated Γ by SF model and by hybrid SC/SF model as a function of I at pH of 4.0 and 6.3. Measured results are also shown. Simulation conditions same as Tables 1 and 2. For the hybrid SC/SF model values of $\chi_s^{\text{(hyb)}}$ are based on reaction 6. A value of 5.6 kJ is used as a baseline to fit Γ at pH 8.0 and I of 0.01. f_0 and f_1 are calculated similar to Figures 3b,d. (b) Interactions between hematite surface sites and PGUA segments as a function of I at pH 4.0. (c) Interactions between hematite surface sites and PGUA segments as a function of I at pH 6.3.

A replacement of water molecules on the surface by the adsorbing ligand is involved in reactions 13 and 14. In studying the adsorption of salicylic acid ($\text{C}_6\text{H}_4(\text{OH})\text{COOH}$) on illite with attenuated total reflection-Fourier transform infrared spectroscopy (ATR-FTIR) measurements and molecular orbital calculations, Kubicki et al. (34) proposed a similar mechanism in which a ligand replaces a water molecule on a surface.

Effects of Ionic Strength. Measured and simulated values of Γ are shown in Figure 5a as functions of I at two different pHs (4.0 and 6.3). A broad range of ionic strengths is covered in this test so that it can be applied to aquatic environments having different ionic strengths, such as rivers, lakes, and estuaries. Simulated results from both the SF and hybrid SC/SF models are included. For the hybrid model, values of $\chi_s^{\text{(hyb)}}$ are based on reaction 6 with the same baseline as used in Figure 2 (5.6 kJ at pH 8.0 and I of 0.01).

Measurements of Γ increase with increasing I at both pHs. Similar behavior has been found experimentally in other studies of polyelectrolyte adsorption on oxide surfaces (4, 20, 21). At pH 4.0, using a constant χ_s of 2 kJ does not predict the enhanced effect of I on Γ accurately. Use of other

values of χ_s yields a similar trend; predicted Γ increases only slightly with increasing I . At this same pH, a better prediction is obtained with the hybrid model; Γ predicted by the hybrid model increases with increasing I somewhat more than with the SF model. However, the hybrid model overestimates Γ at low I and underestimates it at high I . At pH 6.3, the hybrid model exhibits similar predictions as the SF model. However, both the hybrid model and the SF model underpredict Γ at high I at this pH.

Underprediction of the enhanced effect of I on adsorption may be due to the fact that solvent quality becomes poorer (χ increases) as I increases (21, 22). Here Γ represents the Flory-Huggins interaction parameter between PGUA segment and water molecule. The causes of the influence of electrolytes on solvent quality are still not well understood. This change in solvent quality with I is not considered in the simulations and may contribute to the underprediction of Γ at high I .

The overestimation of Γ at pH 4.0 and at low I may be due to an error in the degree of dissociation of PGUA calculated by the model. A $\text{p}K_a$ of 3.92 was used to calculate the degree of dissociation for PGUA, which agrees well with the titration results (Figure 3c) of PGUA in the bulk solution at I of 0.01 but overpredicts f_1 at lower ionic strength. This can overestimate the electrostatic attraction between charged PGUA segments and surfaces and may then overestimate Γ at low I .

The contributions of electrostatic and specific interactions between surface sites and polyelectrolyte segments are estimated (Figure 5b,c). Since both σ_0 and σ_p increase with increasing I (Figure 3a,c), one may expect that χ_s^{elec} would increase with increasing I . However, it is found that χ_s^{elec} decreases with increasing I at the two pHs. This is due to the screening effect of electrolyte ions. $\psi(1)$ (not shown) is reduced as ionic strength increases, even though σ_0 for hematite increases with increasing ionic strength.

At pH 4.0, $\chi_s^{\text{(hyb)}}$ increases with increasing I . This arises mainly from an increase in f_1 as I increases. This means that ionic strength affects polyelectrolyte adsorption not only through its effects on electrostatic interactions but also through its influence on specific interactions between polyelectrolyte functional groups and surface sites. The sum of $\chi_s^{\text{(hyb)}}$ and χ_s^{elec} fluctuates around 6 to 7 kJ. The increases in Γ with increasing I are probably due to the screening effects of electrolytes. Increasing I reduces the electrostatic repulsion among charged PGUA segments and promotes adsorption. Without a consideration of the influence of ionic strength on specific interactions (e.g., the present SF model), the predictions of Γ remain almost unchanged with increasing ionic strength (Figure 5a). With additional change in specific interaction as described by the hybrid model, predictions of Γ increase with increasing I ; agreement with the measured trends is improved compared with the unmodified SF model. However, the result is a net balance among all favorable (including both electrostatic and nonelectrostatic) and unfavorable effects.

At pH 6.3, $\chi_s^{\text{(hyb)}}$ for PGUA adsorbed on hematite remains almost unchanged with increasing ionic strength in the range from 0.0003 to 0.01 (Figure 5c). This is because the decrease in $>\text{MeOH}$ surface groups as I increases is balanced with an increase in L^- species. However, $\chi_s^{\text{(hyb)}}$ decreases from 4.9 to 4 kJ as ionic strength increases from 0.01 to 0.18. This reduction in $\chi_s^{\text{(hyb)}}$ is due to the reduced availability of active surface sites ($>\text{MeOH}$) as ionic strength increases. The sum of $\chi_s^{\text{(hyb)}}$ and χ_s^{elec} decreases with increasing I (Figure 5c). However, Γ increases with increasing I . This reflects the importance of intra- and intermolecular screening effects among adsorbed polyelectrolyte segments as I increases; the decrease in the combined adsorption energy between surface sites and PGUA segments with increasing I is overcompensated.

sated by the reduction in electrostatic repulsions among charged PGUA segments.

Concluding Remarks

The hybrid SC/SF model contributes to a better quantitative understanding of the adsorption process for weak polyelectrolytes and NOM on metal oxide surfaces. It provides a better prediction of the adsorption data over a broad range of solution conditions than present approaches based on a single constant value of χ_s . This broad range of solution conditions includes a wide range of pHs so that both similarly and oppositely charged cases are covered. It also includes a wide range of ionic strengths so that different aquatic systems are covered. This comprehensive test enables the hybrid model to be applied to different aquatic environments under different situations. Accurate description of adsorption data with the hybrid SC/SF model provides useful information about the adsorption process. Important information includes the adsorption reaction and the contributions of electrostatic and chemical interactions to the adsorption. A potential application of the hybrid model in future is to relate predicted adsorbed conformations to the effects of adsorbed polyelectrolytes including natural organic matter on surface properties of particles and, for example, colloidal stability.

Acknowledgments

This research was supported by the U.S. National Science Foundation under Grants BCS-9112766 and BCS-9708520, by the U.S. Environmental Protection Agency under Grant R 812760010, and by the U.S. Office of Naval Research under Grant N00014-92J-1811. The authors thank Professor Alan Stone and Professor Hugh Ellis for valuable comments and suggestions.

Symbols

e	elementary charge (1.902×10^{-19} coulomb)
f_L	the fraction of soluble polyacid species that is dissociated (negatively charged) (dimensionless)
f_1	the fraction of proton reactive surface species that is positively charged (dimensionless)
f_0	the fraction of proton reactive surface species that is neutral (dimensionless)
f_{-1}	the fraction of proton reactive surface species that is negatively charged (dimensionless)
k	Boltzmann constant (1.38×10^{-23} J/K)
M	number of layers in lattice model
pH_{pzc}	point of zero charge of oxide surfaces (dimensionless)
$pK_a(\text{int})$	negative log of (intrinsic) acidity constant of a weak polyacid
$pK_{a1}^s(\text{int})$	negative log of the (intrinsic) first acidity constant of oxide surfaces
$pK_{a2}^s(\text{int})$	negative log of the (intrinsic) second acidity constant of oxide surfaces
r	number of segments of a polyelectrolyte molecule
r_x	number of segments of a molecule x
T	absolute temperature (K)
$u'(i)$	potential energy field of any segment in layer i due to excluded volume effects (kT)
$u_x(i)$	potential energy field of segment x in layer i (kT)

$u_x^{\text{el}}(i)$	potential energy field of segment x in layer i due to the Coulombic interactions between segment x and all other species (kT)
$u_x^{\text{nel}}(i)$	potential energy field of segment x in layer i due to the nonCoulombic interactions between segment x and all other species (kT)
v	valence of a polyelectrolyte segment
v_x	valence of segment type x
w_i	weighting factor for adsorption reaction i (dimensionless)
χ	nonCoulombic interaction parameter between a polyelectrolyte segment and a solvent molecule (kT)
χ_s	nonCoulombic interaction parameter between a polyelectrolyte segment and a surface site (kT)
χ_s^{elec}	electrostatic (Coulombic) interaction between a polyelectrolyte segment and surface sites (kT)
$\chi_s(\text{exp})$	χ_s that can fit the experimental adsorption density (kT)
$\chi_s(\text{hyb})$	χ_s calculated from the hybrid SC/SF model (kT)
χ_{si}	nonCoulombic interaction parameter between a polyelectrolyte segment and a surface site for adsorption reaction i (kT)
$\chi_{s,x}$	nonCoulombic interaction parameter between a segment x and a surface site (kT)
$\chi_{y,x}$	nonCoulombic interaction parameter between a segment y and a segment x (kT)
ϵ_x	relative dielectric permittivity of segment type x (dimensionless)
ϕ_y^b	equilibrium bulk concentration of segment type y (volume fraction)
$\phi_y(i)$	volume fraction of segments y in layer i
Γ	adsorption density of polyelectrolytes (mg/m ²)
σ_o	surface charge density (coul/m ²)
ϕ_p	charge density of a polyelectrolyte (coul/mg C)
$\psi(1)$	electric potential in the first layer (mV)
ψ_o	surface potential (mV)

Literature Cited

- (1) Gebhardt, J. E.; Fuerstenau D. W. *Colloids Surf.* **1983**, 7, 221–231.
- (2) Cohen Stuart, M. A. *J. Phys. France* **1988**, 49, 1001–1008.
- (3) Chibowski, S. *J. Colloid Interface Sci.* **1990**, 140, 444–449.
- (4) Tiller, C. L.; O'Melia, C. R. *Colloids Surf. A* **1993**, 73, 89–102.
- (5) Böhmer, M. R.; Sofi, Y. E. A.; Foissy, A. *J. Colloid Interface Sci.* **1994**, 164, 126–135.
- (6) Hoogeveen, N. G.; Cohen Stuart, M. A.; Fleer, G. J. *J. Colloid Interface Sci.* **1996**, 182, 133–145.
- (7) Ghosh, K.; Schnitzer, M. *Soil Sci.* **1980**, 129, 266–276.
- (8) Vermeer, A. W. P. Ph.D. Dissertation, Wageningen Agricultural University, The Netherlands, 1996.
- (9) Lyklema, J. In *Flocculation, Sedimentation and Consolidation: Proceedings of the Engineering Foundation Conference*; Engineering Foundation: New York, 1985; p 3.
- (10) Schlautman, M. A.; Morgan, J. J. *Geochim. Cosmochim. Acta* **1994**, 58, 4293–4303.
- (11) Tipping, E.; Cooke, D. *Geochim. Cosmochim. Acta* **1982**, 56, 75–80.
- (12) Penners, N. H. G. Ph.D. Dissertation, Wageningen Agricultural University; The Netherlands, 1985.
- (13) Katchalsky, A.; Shavit, N.; Elsenbereg, H. *J. Polymer Sci.* **1954**, 13, 69–84.

- (14) Yang, S. Ph.D. Dissertation, The Johns Hopkins University Baltimore, MD, 1996.
- (15) Scheutjens, J. M. H. M.; Fleer, G. J. *J. Phys. Chem.* **1979**, *83*, 1619–1635.
- (16) Scheutjens, J. M. H. M.; Fleer, G. J. *J. Phys. Chem.* **1980**, *84*, 178–190.
- (17) Böhmer, M. R.; Evers, O. A.; Scheutjens, J. M. H. M. *Macromolecules* **1990**, *23*, 2288–2301.
- (18) Vermeer, A. W. P.; Leermakers F. A. M.; Koopal L. K. *Langmuir* **1997**, *13*, 4413–4421.
- (19) Fleer, G. J.; Cohen Stuart, M. A.; Scheutjens, J. M. H. M.; Cosgrove, T.; Vincent, B. J. *Polymers at Interfaces*; Chapman & Hall: London, 1993.
- (20) Bonekamp, B. C.; van der Schee, H. A.; Lyklema, J. *Croat. Chem. Acta* **1983**, *56*, 695–704.
- (21) Marra, J.; van der Schee, H. A.; Fleer, G. J.; Lyklema, J. In *Adsorption from Solution*; Ottewill, R., Rochester, C. H., Smith, A. L., Eds., Academic Press: London, 1983; p 245.
- (22) Flory, P. J. *Principles of Polymer Chemistry*, Cornell University Press: Ithaca, 1953.
- (23) Silberberg, A. *J. Chem. Phys.* **1968**, *48*, 2835–2851.
- (24) Hjortås, J.; Larsen, B.; Thanomkul, S. *Acta Chem. Scand.* **1974**, *B28*, 689.
- (25) Stumm, W.; Huang, C. P.; Jenkins, S. R. *Croat. Chem. Acta* **1970**, *42*, 223–244.
- (26) Schindler, P. W.; Gamsjager, H. *Kolloid Z. Z. Polym.* **1972**, *250*, 759–763.
- (27) Schindler, P. W.; Furst, B.; Dick, R.; Wolf, P. U. *J. Colloid Interface Sci.* **1976**, *55*, 469–475.
- (28) Stumm, W.; Kummert, R.; Sigg, L. *Croat. Chem. Acta* **1980**, *53*, 291–312.
- (29) Stumm, W. *Chemistry of the Solid-Water Interface*; John Wiley & Sons: New York, 1992.
- (30) Kummert, R.; Stumm, W. *J. Colloid Interface Sci.* **1980**, *75*, 373–385.
- (31) Hiemstra, T.; Van Riemsdijk, W. H.; Bolt, G. H. *J. Colloid Interface Sci.* **1976**, *55*, 469–475.
- (32) Papelis, C.; Hayes, K. F.; Leckie, J. O. *HYDRAQL*; Stanford University: Stanford, California, 1988.
- (33) Biber, M. V.; Stumm, W. *Environ. Sci. Technol.* **1994**, *28*, 763–768.
- (34) Kubicki, J. D.; Itoh, M. I.; Schroeter, L. M.; Apitz S. E. *Environ. Sci. Technol.* **1997**, *31*, 1151–1156.
- (35) Nordin, J.; Persson, P.; Laiti, E.; Sjöberg, S. *Langmuir* **1997**, *13*, 4085–4093.

Received for review March 13, 1998. Revised manuscript received June 30, 1998. Accepted June 30, 1998.

ES9802450